ORIGINAL ARTICLE

Functional Characterization of the Epidermal Cholinergic System *In Vitro*

Hjalmar Kurzen[1], Carmen Henrich[1], Dirk Booken[1], Nina Poenitz[1], Alexei Gratchev[1], Claus-Detlev Klemke[1], Monika Engstner[2], Sergij Goerdt[1] and Nicole Maas-Szabowski[3]

The aim of this study was to analyze the influence of cholinergic and anticholinergic drugs on epidermal physiology using organotypic cocultures (OTCs). Blocking of all acetylcholine receptors (AChRs) by combined treatment with mecamylamine and atropine or treatment with strychnine (blocking α9nAChR) for 7–14 days resulted in a complete inhibition of epidermal differentiation and proliferation. Blockage of nicotinic (n)AChR with mecamylamine led to a less pronounced delay in epidermal differentiation and proliferation than blockage of muscarinic (m)AChR with atropine, evidenced by reduced epithelial thickness and expression of terminal differentiation markers like cytokeratin 2e or filaggrin. In OTCs treated with atropine, mecamylamine, or strychnine, we could demonstrate intracellular lipid accumulation in the lower epidermal layers, indicating a severely disturbed epidermal barrier. In addition, we observed prominent acantholysis in the basal and lower suprabasal layers in mecamylamine-, atropine-, and strychnine-treated cultures, accompanied by a decreased expression of cell adhesion proteins. This globally reduced cell adhesion led to cell death via intrinsic activation of apoptosis. In contrast, stimulation of nAChR and mAChR with cholinergic drugs resulted in a significantly thickened epithelium, accompanied by an improved epithelial maturation. In summary, we show that epidermal AChR are crucially involved in the regulation of epidermal homeostasis.

INTRODUCTION

The epidermis is a highly specialized stratified epithelium that functions to protect the body from physical and chemical damage, infection, dehydration, and heat loss. To achieve this goal, a protective, semipermeable barrier is formed, the stratum corneum. To maintain this critical barrier, the epidermis undergoes constant renewal and repair. Keratinocytes undergo a program of terminal differentiation expressing a set of structural proteins, keratins, that assemble into filaments and function to maintain cell and tissue integrity. Two types of cell adhesion structures, desmosomes and hemidesmosomes, function to connect the keratin cytoskeleton to the cell surface. In concert with adherens junctions and tight junctions that are connected to the actin filaments, they mediate epidermal cell adhesion and regulate the tightness of the epidermal barrier. Epidermal differentiation, cell adhesion, and barrier formation can be influenced by various factors such as calcium ions, vitamin A or D, growth hormones, or cytokines (Fuchs, 1990; Anderson and van Itallie, 1995; Presland and Jurevic, 2002; Segre, 2003). A recently recognized player in the orchestra of epidermal physiology is the extraneuronal cholinergic system. It has been shown to influence various cell functions of resident skin cells such as terminal differentiation and barrier formation, sweat and sebum secretion, as well as microcirculation. It is firmly established that human keratinocytes as well as endothelial cells synthesize and degrade acetylcholine (ACh) that acts via the muscarinic (mAChRs) and nicotinic receptors (nAChRs) either autocrine or paracrine on the surrounding cells like fibroblasts or melanocytes (Smith *et al.*, 1992; Grando, 1997; Kirkpatrick *et al.*, 2003; Kurzen and Schallreuter, 2004). Hitherto, five molecular subtypes of mAChRs have been identified in keratinocytes, melanocytes, and fibroblasts. These receptors are single-subunit transmembrane glycoproteins. The M_2 and M_4 receptors are coupled to G-proteins of the G_i family leading to inhibition of cAMP synthesis via adenylyl cyclase. The M_1, M_3, and M_5 subtypes are coupled to the Gq class of the G-proteins acting on downstream signals such as phospholipase C or D, consequently regulating intracellular calcium levels. The mAChRs have been mapped to different layers of the epidermis.

[1]Department of Dermatology, University Medical Center Mannheim, University of Heidelberg, Mannheim, Germany; [2]Department of Dermatology, University of Heidelberg, Mannheim, Germany and [3]Division of Carcinogenesis and Differentiation, German Cancer Research Center, Heidelberg, Germany

Correspondence: Dr Hjalmar Kurzen, Department of Dermatology, Venereology and Allergology, University Medical Center Mannheim, Ruprecht-Karls University of Heidelberg, Theodor-Kutzer-Ufer 1-3, Mannheim D-68135, Germany.
E-mails: hjalmar.kurzen@haut.ma.uni-heidelberg.de; hjalmar.kurzen@nexgo.de

Abbreviations: ACh, acetylcholine; DP, desmoplakin; Dsc, desmocollin CK, cytokeratin; Dsg, desmoglein; GAPDH, glyceraldehyde-3-phosphate dehydrogenase; HDF, human dermal fibroblast; IF, immunofluorescence; LDH, lactate dehydrogenase; mAChR, muscarinic acetylcholine receptor; nAChR, nicotinic acetylcholine receptor; OTC, organotypic coculture; PG, plakoglobin; RT-PCR, reverse transcription-PCR

However, the exact functional roles of the muscarinic receptors need yet to be demonstrated (Grando *et al.*, 1995b; Ndoye *et al.*, 1998; Buchli *et al.*, 2001; van Koppen and Kaiser, 2003; Kurzen *et al.*, 2004). Human nAChRs are composed of different subunits, that is, α1–α10, β1–β4, γ, δ, and ε, which can be combined to pharmacologically distinct pentameric ion channels. The α1, β1, and δ chains form heteropentamers present at the neuromuscular junction together with the γ (fetal phenotype) and ε (adult phenotype) chains. The neuronal heteropentamers that contain the α3 subunit together with other subunits are also termed α3*-nAChR. The α7 and α9 subunits form homopentamers and are mainly gating calcium, whereas the α3*-nAChR is permeable to both sodium and potassium (Seguela *et al.*, 1993; Millar, 2003). It has been suggested that α9 subunits may form heteromeric nAChR together with α10 subunits (Elgoyhen *et al.*, 1994; Sgard *et al.*, 2001). Depending on their subunit composition, the nAChR show different affinities to ACh, choline, and other cholinergic compounds like nicotine. Although α2-, α4-, α6-, and β3-nAChR have never been demonstrated in human skin, several studies have identified the presence of α3-, α5-, α7-, α9-, α10-, β2-, and β4-nAChR. In addition, the presence of β1-nAChR mRNA and protein was shown only recently (Grando *et al.*, 1995b; Nguyen *et al.*, 2001; Arredondo *et al.*, 2002; Kurzen *et al.*, 2004).

Pharmacological stimulation of the α3*-nAChR has been shown to enhance cell aggregation, cell contact formation, and lateral cell migration (Grando *et al.*, 1995a). A central, calcium-dependent role in terminal differentiation and apoptosis has been suggested for the α7-nAChR, based on cell culture experiments of keratinocyte monolayers. In addition, α7-nAChR knockout mice have a highly proliferative, thickened epidermis with delayed terminal differentiation (Arredondo *et al.*, 2002). However, also other nAChR seem to be involved in the regulation of epidermal barrier formation as indicated by the pharmacological profile reported to enhance a process named ''apoptotic'' secretion. A combination of antimuscarinic and nicotinergic compounds was shown to be required, suggesting a regulatory role also for mAChR or for the α3*- and α9-nAChR (Nguyen *et al.*, 2001).

The role of AChR in the regulation of epidermal cell adhesion has been a controversial issue especially as regards to the role of the cholinergic system in the pathogenesis of the autoimmune blistering skin disease pemphigus vulgaris (Nguyen *et al.*, 1998; Grando *et al.*, 2001; Stanley *et al.*, 2001). In contrast to the current dogma favoring an exclusive role of the desmosomal cadherin desmoglein 3 (Dsg3) in the pathogenesis of pemphigus vulgaris (Amagai *et al.*, 1991; Schmidt *et al.*, 2000; Hertl and Veldman, 2001; Amagai, 2003), there have been several reports on the presence of autoantibodies against cholinergic receptors in the serum of up to 85% of these patients (Nguyen *et al.*, 2000a). In addition, both the desmosomal and classical cadherins can be upregulated by cholinergic substances like carbachol, whereas their phosphorylation has been shown to be promoted by pemphigus vulgaris IgG. This finding has prompted clinical trials reporting a beneficial effect of nicotine or ACh-esterase inhibitors on the clinical course of pemphigus vulgaris. Another central point in this line of evidence was the observation that, on the one hand atropine and mecamylamine, inhibitors of AChR, can induce acantholysis *in vitro* and that, on the other hand, nicotine and muscarine are able to reverse acantholysis induced by pemphigus serum on keratinocyte monolayer cultures. However, the exact mechanism of the observed effects has never been clarified nor have the AChR involved in keratinocyte adhesion been pinned down convincingly. One recent study suggested a central role for the α3*-, α9-, and M_3 AChR in this process (Nguyen *et al.*, 2000b, 2004a, b; Grando, 2004).

The goal of this study was to examine the influence of common cholinergic compounds that are partly in clinical use, on epidermal physiology. In an attempt to approach the physiological situation in human skin and in contrast to previous experiments using keratinocyte monolayers, we used organotypically cultured primary keratinocytes as a three-dimensional epidermis model. We provide functional evidence for a crucial role of several epidermal AChR subtypes in the regulation of epidermal barrier formation, terminal differentiation epidermal cell adhesion, and apoptosis.

RESULTS

Control OTC correspond to normal epidermis with respect to morphology and AChR expression

On the day of the organotypic coculture (OTC) airlift, keratinocytes had grown for 2 days submerged on the fibroblast containing collagen gel. On histological examination, a two- to three-layered non-keratinizing epithelium is formed. After 5 days in culture, the first signs of differentiation became visible with the upper layers flattening and markers of terminal differentiation like cytokeratin (CK)1/10 and Ck2e becoming positive. After 7 days, these markers became more prominent and a stratum corneum became detectable. At the same time, basement membrane components are formed and the epithelium becomes firmly anchored on the collagen gel. After 12–14 days, the epidermis is multilayered and the stratum granulosum and corneum are fully developed (Figure 1a).

As a prerequisite for the possible action of cholinergic compounds, we examined the expression of AChR in OTC by immunofluorescence (IF) and compared their expression with normal epidermis. In mature untreated control OTC, we found all AChR examined (α3, α7, α9, m1, m3, and m5) in an epidermis-like pattern (Figure 2a–e). Performing quantitative real-time reverse transcription (RT)-PCR analysis, we examined the quantity of a α9nAChR mRNA (relative to glyceraldehyde-3-phosphate dehydrogenase (GAPDH) mRNA) in OTCs at different time points. In relation to normal human skin, on day 0 α9nAChR mRNA was found increased 2-fold, 77-fold on day 5, and 166-fold on day 10 (not shown).

Cholinergic antagonists severely interfere with keratinocyte adhesion and differentiation

We first wanted to know whether AChR are needed for the development of a normal epithelium. We therefore blocked
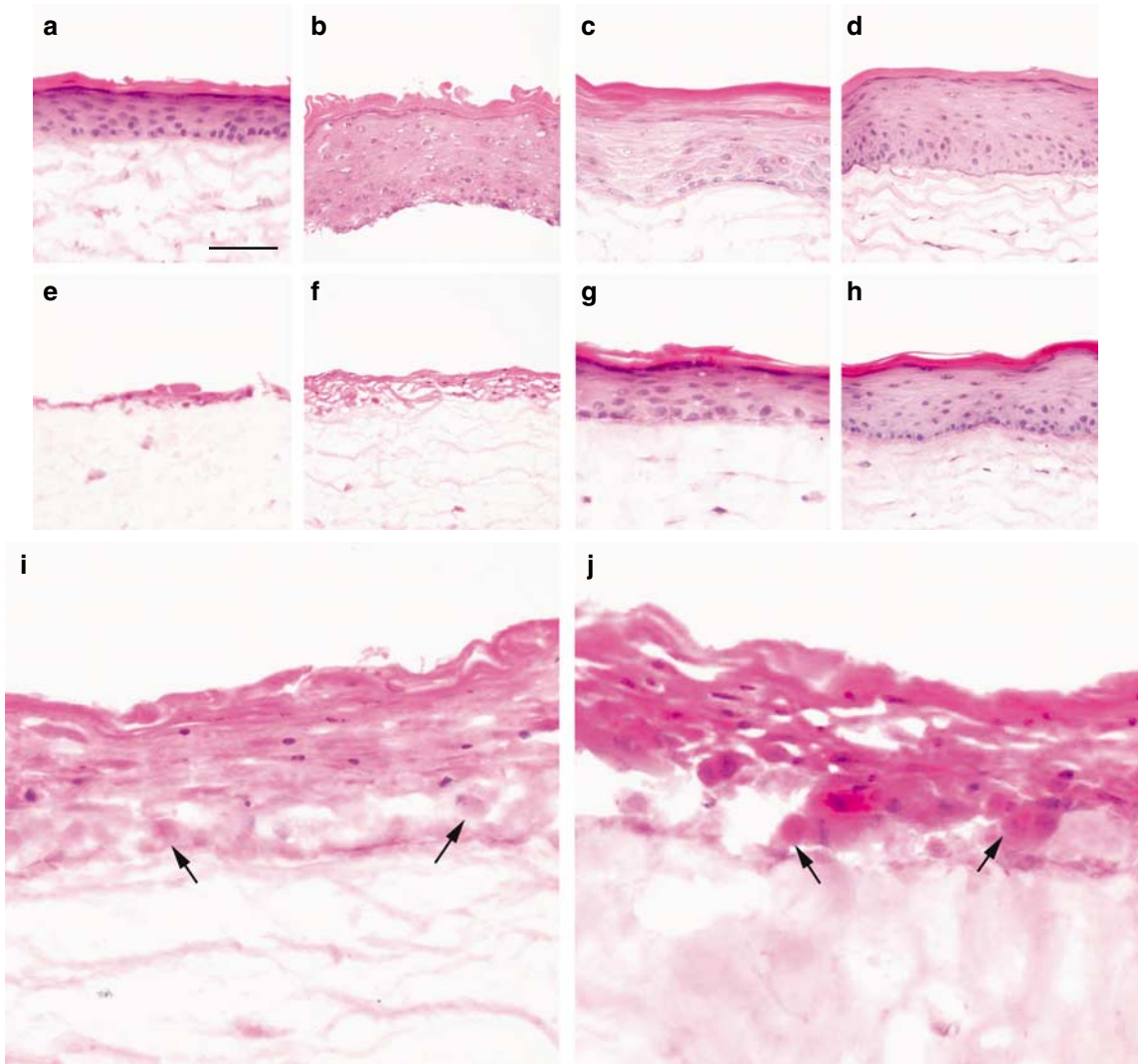
Figure 1. **OTC morphology.** HE staining of untreated organotypic cocultures (**a**) (control OTC), (**b**) OTC treated with nicotine (nicOTC), (**c**) muscarine (muscOTC), (**d**) carbachol (carbaOTC) (**e**) mecamylamine and atropine (mec/atropOTC), (**f**) strychnine (stryOTC), (**g**) α-bungarotoxin (bgtxOTC) (**h**) glycopyrrolate (gpbOTC), (**i**) mecamylamine (mecOTC), and (**j**) atropine (atropOTC). All substances were used in 1 mM concentrations over 10 days after air-lifting. Note that stimulation of (**b–d**) AChR leads to a significantly increased thickness of the obtained epithelium. (**e**) Inhibition of all AChR by combined treatment with atropine and mecamylamine completely inhibits formation of a multilayered epithelium. (**f**) Inhibition of α9-nAChR by strychnine significantly inhibits epidermal maturation and causes acantholysis. Inhibition of nAChR by (**i**) mecamylamine or predominant inhibition of mAChR by (**j**) atropine causes acantholysis in the lower epidermal layers (arrows). α-Bungarotoxin promotes epidermal differentiation without increase in epidermal thickness; (**i**) there is a prominent granular layer. (**h**) Glycopyrrolate interferes with the maturation of the epidermal barrier in the upper epidermal layers. Note the disturbed architecture suggesting a desynchronization of the differentiation process. Bar = 100 μm.
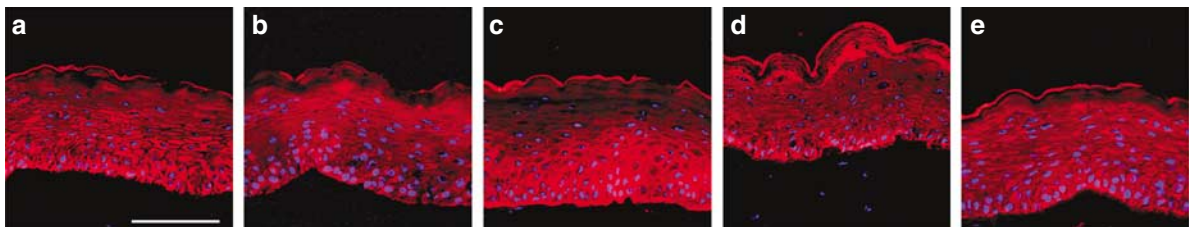

Figure 2. **Differentiation-specific AChR subunit expression in control OTCs.** Untreated OTCs cultured for 12 days. (**a**) IF analysis reveals presence of α3nAChR in the basal layers, (**b**) whereas α7nAChR can be detected in the upper spinous and granular layers. (**c**) Like in the epidermis, α9nAChR are present in the basal in lower suprabasal layers. (**d**) M_3 and (**e**) M_5 immunoreactivity is detectable mainly in the basal cells. Bar = 100 μm.

all AChR by culturing the OTC in the presence of mM concentrations of mecamylamine and atropine (mec/atrop-OTC). In doing so, a functional multilayered epithelium did not develop in our system (Figure 1). In order to exclude toxic and unspecific effects, we determined the concentration of lactate dehydrogenase (LDH) in the OTC supernatant. Compared to control cultures, no significantly increased LDH concentration could be observed in the supernatant.

In the next step, we applied anticholinergic substances with different AChR subtype selectivity and compared the obtained effects. Using mecamylamine (mecOTC), atropine (atropOTC), and strychnine (stryOTC), we obtained functional epithelia, albeit with significantly altered properties as compared to control: there was a prominent acantholysis in the lower suprabasal layers and a significantly delayed epidermal differentiation and with the exception of mecamylamine also a significant reduction of the epidermal thickness. Similar changes could not be observed after OTC culture in the presence of α-bungarotoxin (α-bgtxOTC), hexamethonium (hexaOTC), *d*-tubocurarine (curOTC), or glycopyrrolate (gpbOTC). However, comparing relative epithelial thickness, atropOTC, stryOTC, bgtxOTC, and gpbOTC were significantly thinner than control, whereas mecOTC, hexaOTC, and curOTC did not show any significant change in thickness (Figure 3). In addition, bgtxOTC showed a marked hypergranulosis and gpbOTC displayed a disturbed architecture in the suprabasal cell layers, indicating a desynchronization of the stratification and differentiation process (Figure 1). Again, no increase of LDH in the culture medium could be demonstrated except for strychnine, where we observed a slightly elevated LDH concentration at 1 mM (not shown).

OTC thickness is increased by cholinergic agonists
We wanted to find out whether stimulation of all the AChR, the nAChR, or the mAChR would lead to different effects on epidermal thickness. In nicOTC, we found the most significant increase in epithelial thickness as compared to control OTC, whereas muscOTC and carbOTC showed only
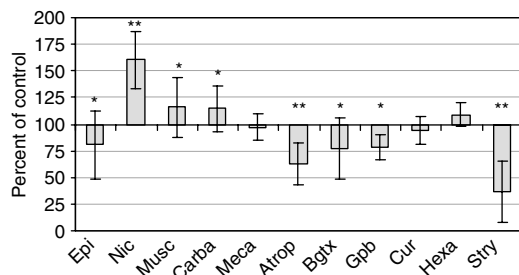

Figure 3. **Epithelial thickness.** The thickness of epidermal living layers was assessed by measuring at three different representative parts of three experiments. The obtained data were pooled. Mean and standard deviation were determined using a Student's *t*-test. Treatment with muscarine and carbachol leads to a slight but significant (*P<0.05) increase in epithelial thickness, whereas nicotine has a much more pronounced effect (**P<0.0001). In contrast, treatment with atropine and strychnine significantly reduce epidermal thickness. All other substances applied, in particular mecamylamine, did not change epithelial thickness significantly.

a slight, but significant increase (Figure 3). Cytotoxic effects were not observed using the LDH release assay.

Expression of markers of terminal differentiation in OTC
In order to characterize the degree of maturation of the different OTCs, we used antibodies against CKs. In fully developed control OTC, all markers of terminal differentiation applied (CK2e, CK5, CK10, and filaggrin) corresponded to normal epidermis, except the activation marker CK6, which remained positive at all times. Ck2e and filaggrin were coexpressed in the granular and uppermost spinous layers indicating maturation and cornification of the epithelium (Figure 4). On day 5, control OTC, nicOTC, muscOTC, and carbOTC only showed a weak CK2e and filaggrin staining which became considerably more intense and extended after 7 days. In contrast to the agonist-treated OTC, in the mecOTC, atropOTC, and stryOTC, CK2e remained completely negative at all times. In the same specimens, filaggrin showed a weak cytoplasmic staining in the cells of the granular layer. A weak CK10 expression could be detected in mecOTC and atropOTC, whereas in stryOTC CK10 could not be detected. CK6 staining intensity was most pronounced in atropOTC, whereas in all other OTC the staining was comparable to control OTC. A weak CK19 staining could be detected in stryOTC and single cells of atropOTC, whereas all other OTCs remained negative (Figure 4). CK5 remained restricted to the basal layer under all conditions (not shown).

Changes in cell adhesion
Desmosomal proteins. In control OTC, antibodies against the desmosomal proteins desmoplakin (DP), plakoglobin, Dsg1, and desmocollin (Dsc)1 produced an epidermis-like intercellular staining pattern. Dsg3 reactivity was extended to all layers and Dsc2 was reduced to the lowermost suprabasal layers, as opposed to normal epidermis, where both proteins are expressed in a gradient from the basal to the upper spinous layers (Kurzen *et al.*, 1999). In nicOTC, muscOTC, and carbOTC, the staining pattern remained unchanged but the staining intensity of all desmosomal antibodies was slightly more intense than in control OTC. In atropOTC, the first noticeable change as compared to control occurred on day 5: there was a marked cytoplasmic staining for plakoglobin (not shown), Dsg3, and Dsc2, whereas Dsg1 could be detected only in the uppermost layers, in part also in the cytoplasm. On day 7, with the appearance of acantholysis, all desmosomal proteins displayed a drastically reduced staining intensity. Especially in the acantholytic cells, the staining intensity did not surpass background levels. Only the cells directly neighboring the acantholytic zone showed a weak cytoplasmic staining. Dsc1 could not be detected. In mecOTC, the changes on day 5, preceding the onset of acantholysis, were not as marked as in atropOTC. From day 7, however, acantholysis was pronounced and the changes in desmosomal protein expression could not be distinguished from the atropOTC specimens. In the very thin, immature epithelium of stryOTC on day 5, all antibodies displayed a diffuse cytoplasmic staining. From day 7, the acantholytic epithelium showed a weak cytoplasmic DP and Dsg3
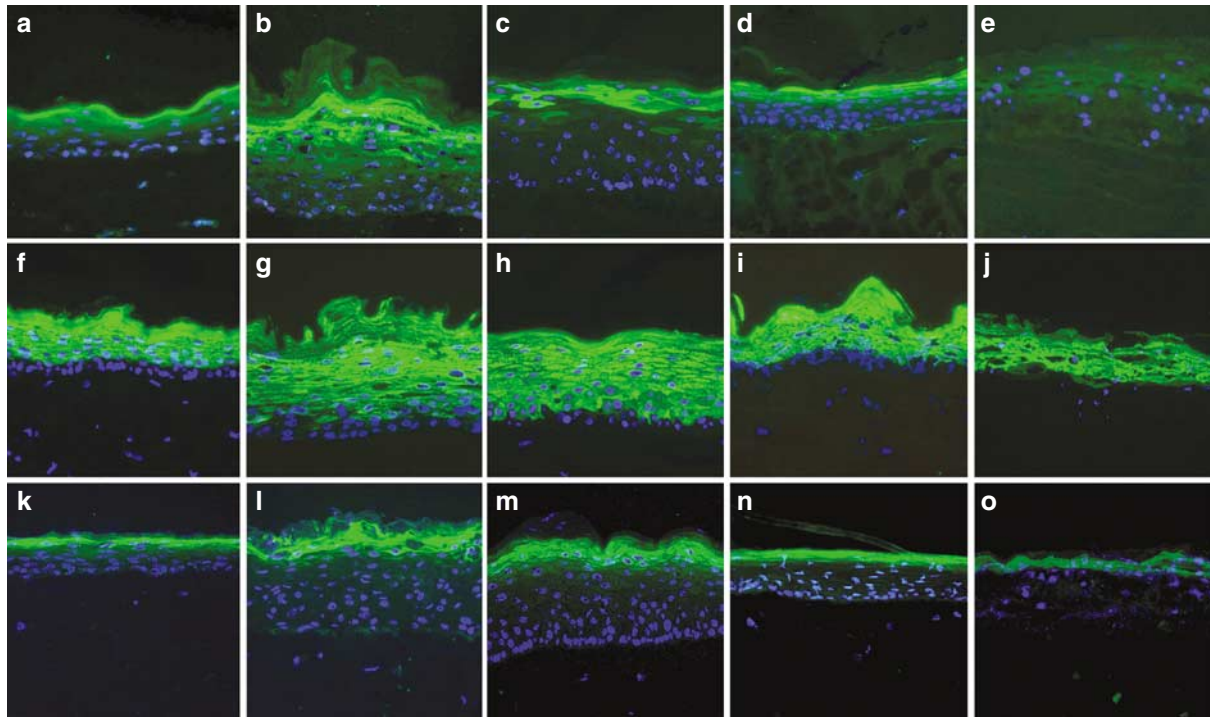
Figure 4. Markers of terminal differentiation in OTC. In control OTC (day 10), (**a**) CK2e expression in the upper epidermal layers is slightly less intense than in normal epidermis, whereas (**f**) CK10 and (**k**) filaggrin expression correspond to normal epidermis. In (**b**) nicOTC and (**c**) carbOTC, (**b**, **c**) Ck2e and (**l**, **m**) filaggrin are strongly expressed in the granular and uppermost spinous layers indicating increased maturation and cornification of the epithelium. (**g**) Ck10 staining pattern in nicOTC seems less compact than in (**f**) control and (**h**) carbOTC. Treatment of OTCs with α-bungarotoxin did not change (**d**) CK2e, (**i**) CK10, or (**n**) filaggrin expression significantly compared to (**a**, **f**) control. In contrast, in the (**e**) mecOTC, CK2e remained completely negative at all times whereas only a weak (**j**) CK10 and (**o**) filaggrin expression could be detected. Bar = 100 μm.

Table 1. Summary of expression patterns in fully developed OTCs (10 days in culture)

	DP	PG	Dsg1	Dsg3	Dsc1	Ecad	β-Cat	ZO-1	α6-Int	β1-Int	Lam	Fil	CK2e	CK5	CK10	CK6/16	CK19
Epidermis	++	++	++	++	+	+	ND	+	+	+	+	+	++	+	++	−	−
Control	+	++	++	+	+	+	ND	+	+	+	+	+	(+)	+	+	+	−
Nicotine	+	++	+	++	+	+	+	+	+	+	+	+	+	+	+	+	−
Muscarine	+	++	+	+	+	+	+	++	+	+	+	+	+	+	+	+	−
Carbachol	++	++	++	++	++	++	++	++	+	+	+	+	+	+	+	+	−
Atropine	(+)cp	−	(+)	(+)cp	−	−	(+)	(+)cp	+	+	−	(+)	−	(+)	(+)	++	−
Mecamylamine	(+)cp	−	(+)	(+)cp	−	−	(+)	(+)cp	+	+	−	(+)	(+)	(+)	(+)	+	−
Strychnine	(+)	−	−	(+)	−	−	(+)	−	+	+	−	(+)	−	(+)	−	+	−
d-Tubocurarin	+	++	+	+	−	+	+	+	+	+	+	+	−	+	+	+	−
Hexamethonium	+	++	+	+	−	+	+	+	+	(+)	+	+	+	+	+	+	−
α-Bungarotoxin	+	++	(+)	+	(+)	+	+	+	+	+	+	+	+	+	+	+	−
Glycopyrrolate	+	++	+	+	+cp	+	+	(+)cp	+	+	+	+	−	+	+	+	−

CK, cytokeratin; DP, desmoplakin; Dsc, desmocollin; Dsg, desmoglein; OTC, organotypic coculture; PG, plakoglobin.
Legend: +, positive; ++, strong reactivity; (+), weak reactivity; −, negative; cp, cytoplasmic staining; ND, not done.

staining, whereas all other desmosomal proteins could not be detected. In hexOTC, curOTC, and bgtxOTC, there were no significant differences compared to control OTC. In gpbOTC, the distribution of all desmosomal proteins was markedly altered, with cytoplasmic staining and a chaotic order reflecting a disturbed keratinocyte synchronization (Figure 5, Table 1). Performing quantitative real-time RT-PCR analysis, we could demonstrate a reduction of Dsg3 mRNA (relative to GAPDH mRNA) to 38% of control OTCs in stryOTCs on day 10 (not shown).

Adherens junctions. In normal epidermis and control OTC, nicOTC, muscOTC, and carbOTC, E-cadherin and β-catenin antibodies brightly decorated cell membranes of all living layers. In mecOTC and atropOTC, the staining intensity was slightly reduced on day 5. With the appearance of acantholysis on day 7, E-cadherin and β-catenin turned almost completely negative. In stryOTC, adherens junction protein antibodies produced a diffuse cytoplasmic staining hardly above background levels. In gpbOTC, the E-cadherin and β-catenin antibodies' staining intensity was comparable to control OTC; however, the disturbed epithelial architecture became clearly visible and many cells showed a cytoplasmic staining (Figure 6, Table 1). Performing quantitative real-time RT-PCR analysis, E-cadherin mRNA could not be detected in stryOTCs (not shown).

Tight junctions. The tight junction protein ZO-1 (TJP1) and claudin 4 could be detected in cell membranes of the upper spinous and granular layer of normal epidermis and fully developed control OTC. In immature OTC of day 5, ZO-1

Figure 5. **Distribution of desmosomal cadherins.** Colocalization of Dsg3 (green) and Dsc2 (red) nuclear counterstain with 4′,6-diamidine-2′-phenyl-indole dihydrochloride (blue). In normal epidermis, (**a**) both proteins are expressed in all layers, with a predominance in the basal and spinous layers. In OTCs, maturation goes along with a change of Dsc2 distribution, retracting from the upper layers, whereas Dsg3 expression remains unchanged (**b**) control after 5 days, (**c**) after 10 days. Atropine leads to a redistribution of desmosomal proteins, (**d**) producing a prominent cytoplasmic staining after 5 days and (**e**, arrows) prominent acantholysis after 10 days with significantly reduced staining intensity of all Dsg3 and Dsc2. In contrast, muscarine treatment (**f**, after 5 days) leads to a bright cell membrane staining, not discernable from control OTCs. (**g**) Also mecamylamine significantly alters Dsg3 and Dsc2 expression already on day 5, however, staining is predominantly confined to the cell membrane and not the cytoplasm. (**h**) After 10 days, mecamylamine treatment acantholysis is evident and staining intensity of Dsg3 and Dsc2 is grossly reduced. (**i**) In contrast, in nicOTCs, the distribution pattern corresponds to control. Bar = 100 μm.

and claudin 4 stainings were often weak and cytoplasmic. The most prominent and extended ZO-1 staining, reaching down to the lower suprabasal layers, was obtained in carbOTC, whereas in nicOTC and muscOTC, no significant changes were noted as compared to control OTC. In the same specimens, claudin 4 remained restricted to the upper spinous and the granular layer (Figure 7f–h). In mecOTC, atropOTC, and stryOTC, ZO-1 and claudin 4 staining intensity was strikingly reduced, being restricted to the cytoplasm of the cells in close proximity of the acantholytic zones. Like for the desmosomal proteins, gpbOTC produced a chaotic, mostly cytoplasmic ZO-1 staining (Figure 7e) and led to claudin 4 decorating areas of premature cornification (Figure 7j). In all other OTCs, there was no significant difference as compared to control (not shown).

Basement membrane components
In control OTC, α6- and β1-integrin and laminin appeared on day 5 in the basal cells, from day 7 onwards, there was an epidermis-like linear deposition, indicating the formation of an intact basement membrane. In the nicOTC, muscOTC, and carbOTC, all three proteins were deposited in a similar way. In addition, the β1-integrin antibody decorated the basal and spinous layers of control OTC, nicOTC and carbOTC, and muscOTC. In atropOTC, mecOTC, and stryOTC, α6- and β1-integrin could be detected along the basement membrane, whereas laminin remained negative. Except for a slightly reduced staining intensity of the β1-integrin antibody in hexOTC, there were no significant changes as compared to control under all other conditions (Figure 8).

Induction of apoptosis in OTCs via the intrinsic pathway
After having observed prominent acantholysis in the mecOTC, atropOTC, and stryOTC, we sought to determine whether apoptosis is induced under these conditions. Performing the TUNEL assay, we found significantly increased fluorescence signal intensity and signal distribution in the stratum spinosum and especially in the acantholytic cells of the mecOTC, atropOTC, and stryOTC from day 7 onwards, whereas under all other conditions, especially in mecOTC, atropOTC, and stryOTC examined on day 5, that is, before the onset of acantholysis, no differences could be observed as compared to control OTC. In the same specimens, an antiserum against activated caspase 3 showed prominent staining of the acantholytic cells (Figure 9), whereas under all other conditions, no staining could be observed. Using antibodies against caspase 8, Bax, and CD95, we did not observe any significant staining as compared to sections obtained from patients with pemphigus vulgaris or basal cell carcinomas, which both showed prominent staining of these proapoptotic proteins (not shown).

Premature lipid deposition in "acantholytic" OTCs
A modified Nile red staining was used in order to assess the lipid composition of the stratum corneum and the degree of maturation reached by the organotypic cultures. Normal human skin and diseased skin with perturbed skin barrier (psoriasis, eczema) was used in comparison.
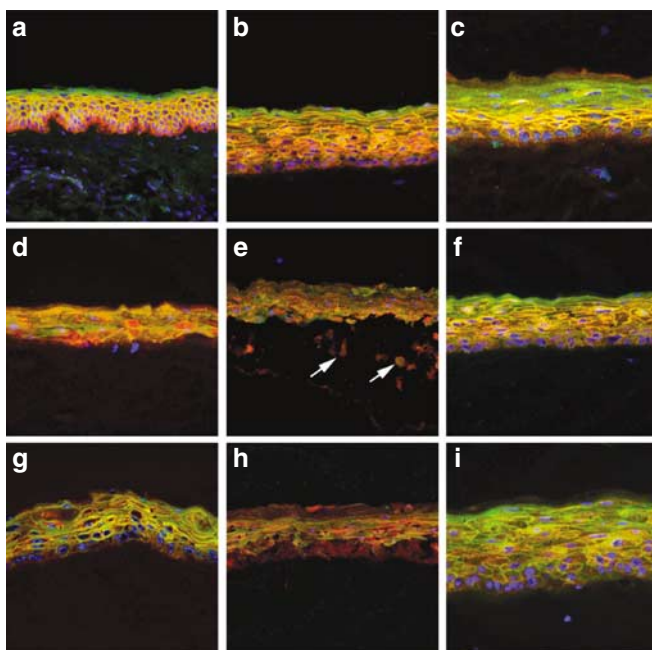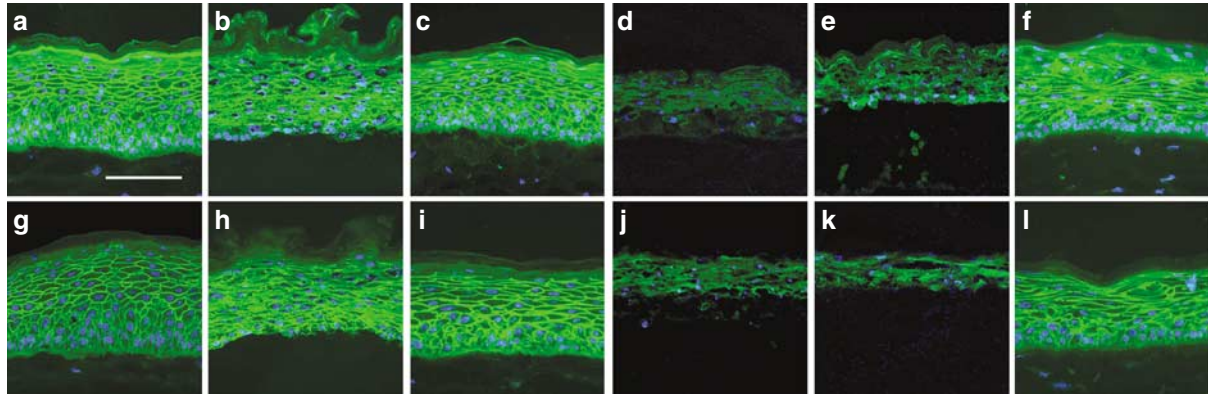
Figure 6. **Distribution of adherens junction proteins.** In (**a**, **g**) control OTC adherens junction proteins examined, namely (**a**) E-cadherin and (**g**) *β*-catenin are broadly expressed in all living epidermal layers. Treatment with (**b**, **h**) nicotine or (**c**, **i**) carbachol leads to a slightly increased signal intensity for (**b**, **c**) E-cadherin and (**h**, **i**) *β*-catenin. In contrast, with the appearance of acantholysis on day 7, after treatment with (**d**, **j**) mecamylamine and (**e**, **k**) atropine, the staining intensity for all adherens junction proteins was markedly reduced. Especially in the acantholytic cells, (**d**, **j**, **e**, **k**) E-cadherin and *β*-catenin turned completely negative. In gpbOTC, (**f**, **l**) the E-cadherin and *β*-catenin antibodies' staining intensity was comparable to control OTC, however, the disturbed epithelial architecture become clearly visible (**f**, **l**, arrows) and many cells showed a cytoplasmic staining. Bar $=100\,\mu m$.
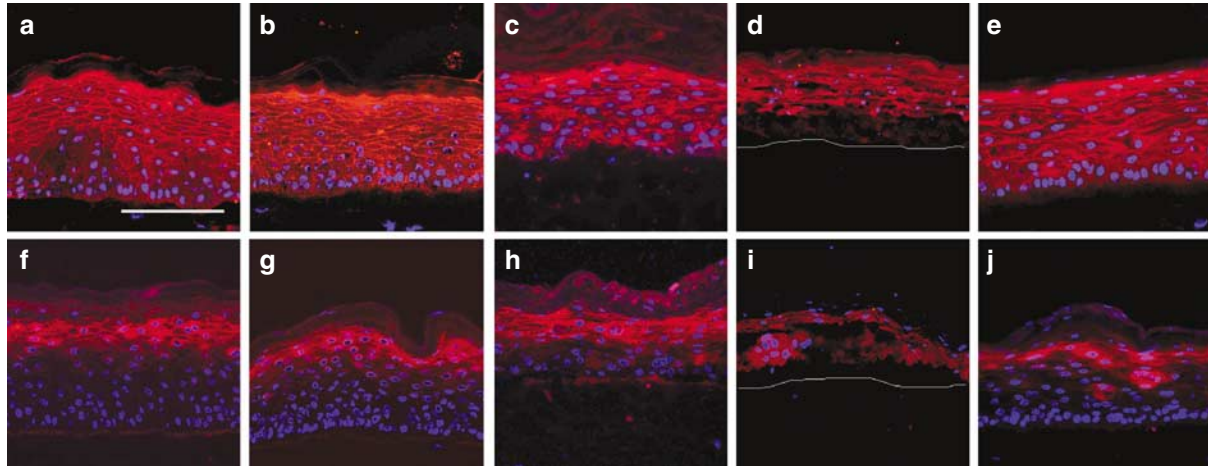

Figure 7. **Distribution of tight junction proteins.** Fully developed OTC treated with (**b**, **g**) carbachol, (**c**, **h**) nicotine, (**d**, **i**) mecamylamine, and (**e**, **j**) glycopyrrolate. ZO-1 could be detected in cell membranes of the upper spinous and granular layer of fully developed (**a**) control OTC whereas (**f**) Claudin 4 remained restricted to the granular cell layer. The most prominent and extended ZO-1 staining reaching down to the lower suprabasal layers was obtained in (**b**) carbOTC and (**c**) nicOTC whereas (**g**, **h**) Claudin 4 did not show a significant change. In (**d**, **i**) mecOTC, ZO-1 and Claudin 4 staining intensity was significantly reduced, being restricted to the cytoplasm of the cells in close proximity of the acantholytic zones. Like for the desmosomal proteins, glycopyrrolate treatment produced a chaotic, in part (**e**) cytoplasmic ZO-1 – and (**j**) Claudin 4 staining. Bar $=100\,\mu\textrm{M}$.

Alkaline extension of the stratum corneum revealed regular "mortar and brick" structure of the stratum corneum of normal skin and untreated organotypic cultures. The first signs of cornification and extracellular lipid deposition were seen 5 days after air lifting; after 10 days, a fully developed stratum corneum displayed intercellular lipid deposition with focal accumulations of lipid droplets. In psoriatic skin, the regular "brick and mortar" structure was severely disturbed, leading to a diffuse non-specific staining. The atropOTC, mecOTC, and stryOTC displayed signs of premature, intracellular lipid production, already in the lowest suprabasal layers, most notably also in the acantholytic cells. In nicOTC, carbOTC, or muscOTC, no premature lipid production was noted, instead, lipids were intensely produced in the stratum corneum. Under all other conditions, no changes were noted as compared to control (Figure 10).

Proliferative activity in OTCs
The proliferative activity of the different OTCs was assessed using an antibody against Ki-67 (Mib-1). In normal epidermis, about 10% of the nuclei in the basal layer are reactive. In immature control OTCs and agonist-treated OTC, there was a slight increase to 10–20%. In the antagonist-treated OTCs up to day 5, we did not detect any significant decrease in the Ki-67 ratio. However, in the mecOTC, atropOTC, and stryOTC, beginning with the onset of acantholysis on day 7, only single Mib-1-positive nuclei could be detected (Figure 11). All other OTCs showed no significant changes compared to control OTC (not shown).
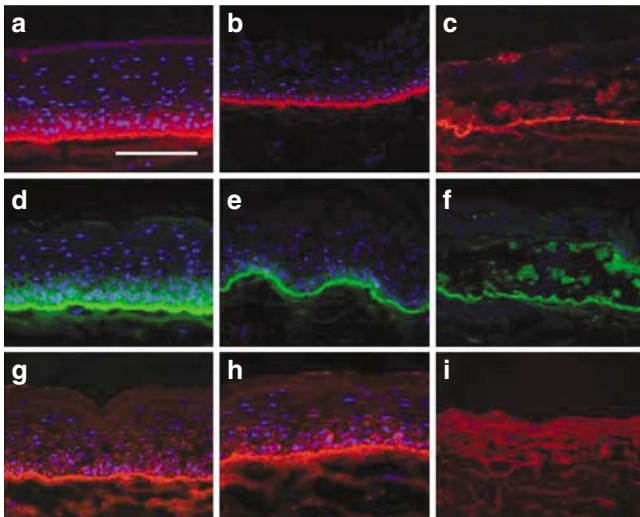
Figure 8. Changes in cell–substrate adhesion. In (**a**, **d**, **g**) control OTC, (**a**) beta-1 and (**d**) alpha-6 – integrin are produced by basal and suprabasal cells indicating a hyperproliferative state with reduced epithelial polarity, (**g**) whereas laminin remains restricted to the basal cells. (**b**, **e**, **h**) In nicotine-treated OTCs, polarity is improved as indicated by retraction of $\beta1$ and $\alpha6$ to the basal cells. Treatment with mecamylamine does not influence (**c**) $\beta1$ and (**f**) $\alpha6$ integrin expression. Both proteins are detectable in a linear pattern below the acantholytic zone. (**i**) In contrast, laminin signal intensity does not surpass background level. Bar $= 100\,\mu m$.

DISCUSSION

After previously having provided a concise phenotypical mapping of AChR present in human skin, our goal was to obtain functional data of AChR stimulation and inhibition in living three-dimensional skin equivalents. The technique of OTCs has been developed and studied in detail by one of us (N.M-S.) and is hence suited to test the impact of cholinergic compounds on various aspects of epidermal physiology. Our first question was whether ACh is needed for epidermal development and survival, at all. Blocking of all AChR, present in control OTC in an epidermis-like distribution (Figure 2), specifically inhibited the formation of an intact epithelium, leaving behind a monolayer of viable, non-differentiated cells, without exerting cytotoxic effects. This observation is well in line with potent antiproliferative effects observed for several nAChR or mAChR blocking compounds in different cell systems (LeSage *et al.*, 1999; Arredondo *et al.*, 2003). In contrast, blocking of the $\alpha7$nAChR has been suggested to enhance proliferative activity in mouse keratinocytes cultured in monolayers (Arredondo *et al.*, 2002), a finding we could not substantiate in our system, most probably because $\alpha7$nAChR were produced only in the last stages of epidermal development, that is, after day 10, along with the formation of a granular layer (Figure 2b). The epithelium formed in the presence of 1 mM strychnine was only two to four cell layers thick without any signs of terminal differentiation. There was a weak expression of CK19, also found in simple epithelia, underlining the lack of observed maturation (Kurzen *et al.*, 1999). As strychnine does also inhibit glycine receptors, we wanted to rule out the possibility that the observed effects were mediated by these ligand-gated
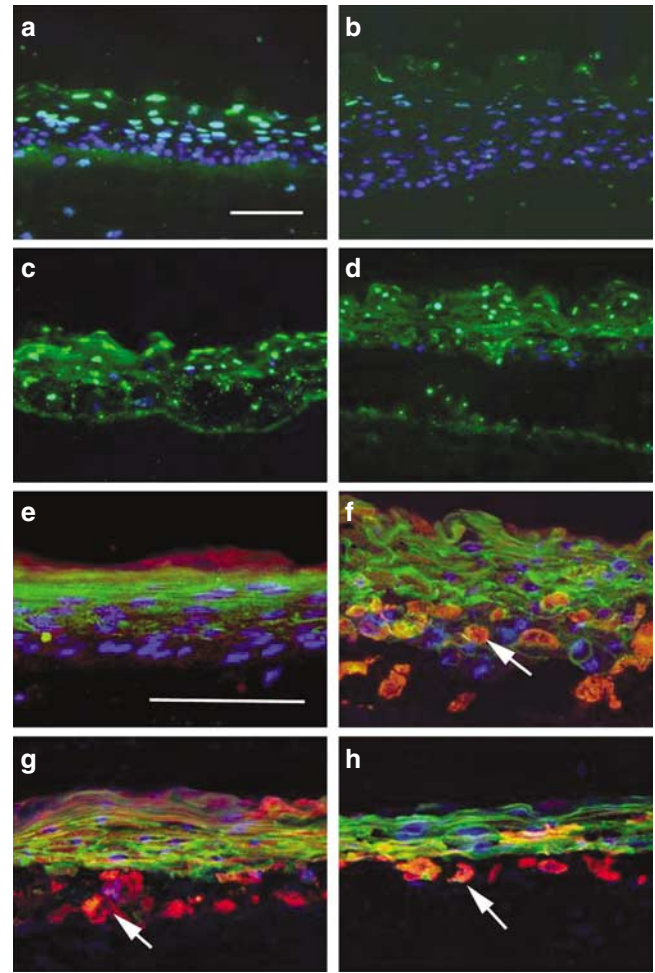

Figure 9. Detection of apoptosis. In order to detect apoptosis, the TUNEL reaction was performed in all OTCs. Blue counterstaining of nuclei with 4′,6-diamidine-2′-phenylindole dihydrochloride, TUNEL signal green. Compared to (**a**) control, (**b**) nicotine does not increase signal intensity in the nuclei in any of the layers. In contrast, even in the granular layer signal intensity seems to be reduced. In (**c**) mecOTC and (**d**) atropOTC, there is a strong increase in signal intensity in all epidermal layers. Activated caspase 3 is a late marker of apoptosis. (**e**–**h**) Double labeling of activated caspase 3 (red), DP (green), and 4′,6-diamidine-2′-phenylindole dihydrochloride (blue). While in (**e**) control OTCs, DP displays a regular labeling and caspase 3 is not detectable, in (**f**) atropOTC, (**g**) mecOTC, and (**h**) stryOTC, there is a prominent activated caspase 3 signal in the acantholytic cells and a weaker signal in the surrounding cells. Note absence of DP in the acantholytic cells (arrows). Bar $= 100\,\mu m$.

chloride channels. Addition of equimolar concentrations of glycine to the stryOTC did not rescue the observed phenotype (not shown). We therefore concluded that the observed strychnine effects were predominantly mediated by inhibition of $\alpha9$nAChR and consequently, $\alpha9$nAChR are crucially involved in the development of a normal, differentiated epidermis. Quantitative analysis revealed a highly significant upregulation of $\alpha9$nAChR mRNA in the course of epithelial maturation in control OTCs underlining its importance for a normal epidermal development.

As second most important finding, we observed prominent acantholysis after treatment with atropine, mecamylamine,

and strychnine. As AChR, especially the α9nAChR, have been suggested to play a role in the pathogenesis of the autoimmune blistering disease pemphigus vulgaris, we wanted to know whether the acantholysis observed in our model corresponds to pemphigus acantholysis or rather other (congenital) acantholytic diseases like Darier's disease. Acantholysis started on day 7 after airlifting. On day 5, acantholysis was not observed but adhesion molecules began

to localize to the cytoplasm. Inhibition of both the ligand-gated ion channels (nAChR) by mecamylamine and blockage of G-protein-coupled receptors (mAChR) lead to similar results, which is quite a stunning observation. As both receptor systems are involved in the regulation of intra-cellular calcium ions (Zia *et al.*, 2000; van Koppen and Kaiser, 2003), we suspected that calcium-dependent adhe-sion molecules might be involved in the observed acantho-lysis. We could confirm this hypothesis by examination of desmosomal and classical cadherins, both of which were dramatically reduced in the IF analysis in the acantholytic OTC. Using quantitative real-time RT-PCR analysis, we could demonstrate that in the strychnine-treated OTCs that were chosen as an example of ''acantholytic'' OTCs, Dsg3 and E-cadherin were significantly downregulated on the mRNA level.

Figure 10. Influence on lipid production. Using Nile red staining with alkaline extension of the stratum corneum, a regular ''mortar and brick'' structure of the stratum corneum of (**a**) normal skin and (**b**) untreated organotypic cultures (**c**) in contrast to psoriasis is revealed. Lipids stain in bright yellow. Note that in normal epidermis and control OTC, there are only single cells showing bright yellow signals in the living layers of the epidermis, whereas in (**b**) psoriasis as well as in (**g**) mecOTC, (**h**) atropOTC, and (**i**) stryOTC already in the lowest suprabasal layers, many keratinocytes display a brightly yellow cytoplasm indicating intracellular accumulation of lipids. In (**d**) nicOTC, (**e**) carbOTC, or (**f**) muscOTC, no premature lipid production was noted, instead, lipids were intensely produced in the stratum corneum. Bar = 100 μm.

In addition, also desmosomal and adherens junction plaque proteins DP, plakoglobin (γ-catenin), β-catenin, and even tight junction proteins like ZO-1 were found signifi-cantly reduced in IF. Our findings of a ''global'' down-regulation of virtually all cell–cell adhesion molecules examined, surpasses the pattern found for pemphigus vulgaris and Darier's disease where single adhesion molecules like Dsg3 and plakoglobin for pemphigus vulgaris or DP for Darier's disease have been found altered (Setoyama *et al.*, 1991; Hashimoto *et al.*, 1995; Aoyama and Kitajima, 1999; Hakuno *et al.*, 2000; Dhitavat *et al.*, 2003). Our results are well in line with previous studies showing phosphorylation (and thus inactivation) of Dsg3, E-cadherin, and β-catenin by atropine in a squamous cell carcinoma cell line and upregulation of Dsg1 and Dsg3 in keratinocyte monolayers by carbachol treatment. Interestingly, mecamylamine did not lead to altered phosphorylation of these molecules in the same system indicating the involvement of different signaling cascades (Nguyen *et al.*, 2003).

Using our model, for the first time, we provide evidence that inhibition of AChR can lead to acantholysis in a three-dimensional *in vitro* epidermis equivalent which closely
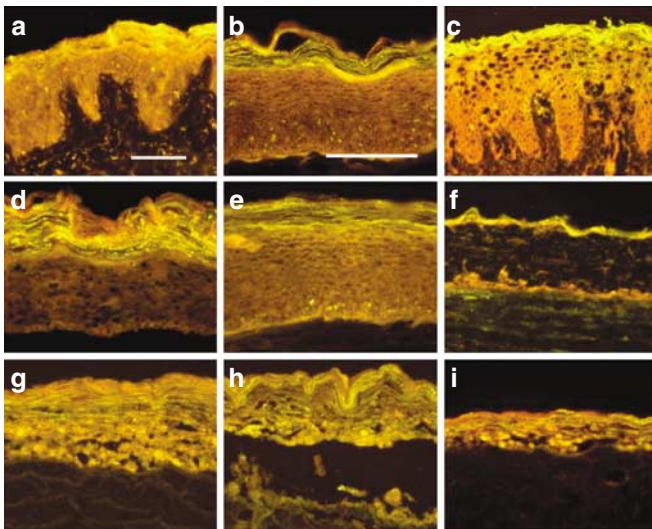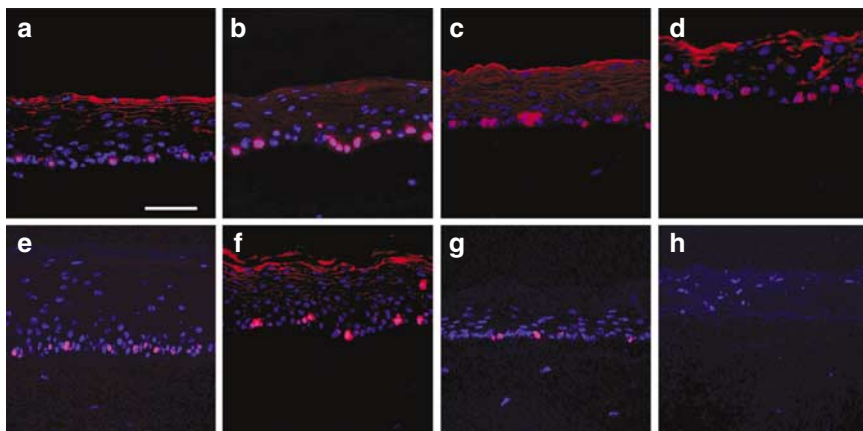

Figure 11. Influence on keratinocyte proliferation. The proliferation marker Ki-67 is detected in 10–20% of nuclei in basal layer of the control OTCs on (**a**) day 5 whereas on (**e**) day 10 only single signal clusters could be detected. Neither (**b**) nicOTC, (**c**) muscOTC, nor (**d**) mecOTC show significantly altered signal ratios on day 5. (carbOTC, **f**) In contrast, on day 10, proliferative activity is still present in the agonist-treated OTCs. (**g**) In α-bungarotoxin-treated OTCs, the signal frequency is comparable to control, (mecOTC, **h**) whereas in the acantholytic OTCs most specimens remained completely negative. Bar = 100 μm.

resembles the *in vivo* situation. In contrast to pemphigus vulgaris, we did not find the typical ''tombstone''- pattern of remaining basal keratinocytes, instead, single basal cells remained attached to the dermis equivalent. This observation can be explained by the rather poor stability of OTCs employing collagen hydrogels as dermal equivalents. In particular, formation of an intact basement membrane is limited, despite the presence of basement membrane components (Stark *et al.*, 2004b). In addition, we observed a reduction of laminin in acantholytic OTCs, adding a further explanation to the observed phenotype.

Biochemical induction of acantholysis has been demonstrated in skin explant cultures by millimolar concentrations of several substances, among which calcium channel antagonists like nifedipine and angiotensin-converting enzyme inhibitors like enalapril (Brenner *et al.*, 1999; Lo Schiavo *et al.*, 1999). Obviously, nifedipine interferes with intracellular calcium homeostasis in keratinocytes thus pointing the way to a common possible mechanism together with the anticholinergic, calcium-reducing effects observed in our system. Our data provide further basis for the clinical use of cholinergic agonists like nicotine or carbachol as antiacantholytic compounds either locally or systemically. As the extraneuronal cholinergic system is also involved in the regulation of inflammatory reactions and cholinergic agonists have shown potent anti-inflammatory capacity, these drugs might be valuable adjuncts to the treatment of pemphigus vulgaris (Grando, 2000; Nguyen *et al.*, 2000a, b, 2004a; Grando *et al.*, 2001).

Like in pemphigus vulgaris, acantholysis in our system was associated with apoptosis, as evidenced by the TUNEL reaction and activated caspase 3. Although the TUNEL reaction showed prominent signals in all layers of the respective epithelia, activated caspase 3 was restricted to the acantholytic cells, thus paralleling the absence of intercellular adhesion molecules. In contrast to pemphigus vulgaris, ''perilesional'' cells did not show caspase 3 activity. Inactivation of adherens junction has been shown to lead to apoptosis in other epithelia and also a very attractive explanation for the apoptogenic mechanism observed in our OTC (Hermiston and Gordon, 1995). Interestingly, neither caspase 8, CD95 nor Bax were upregulated in the acantholytic OTCs, well in line with an intrinsic apoptotic pathway, which is in contrast with the extrinsic pathway in pemphigus vulgaris (Reed, 2000; Wang *et al.*, 2004). We therefore conclude that in our acantholysis model, neither acantholysis nor apoptosis are induced by the same mechanism as in pemphigus vulgaris. Further studies have to show, whether this might be related to our rather broad pharmacological approach or to the lack of specific signaling pathways.

Apoptosis has been shown to be induced by the loss of cell substrate adhesion, a process is also termed anoikis (Frisch and Francis, 1994). With the exception of the slightly reduced basement membrane component laminin, the expression of the cell–matrix adhesion molecules α6- and β1-integrin was intact in the acantholytic OTC, arguing against a major role of cell–substrate adhesion in apoptosis induction in our system.

Interestingly, it has been shown, that activation of mAChR can prevent caspase 2/3 activation by phosphoinositide 3-kinase- and mitogen-activated protein kinase/extracellular signal-regulated kinase-independent pathways. It thus seems plausible that inhibition of mAChR by atropine can induce or promote caspase activation leading to apoptotic cell death, as observed in our system (Leloup *et al.*, 2000). Other pathways of apoptosis regulation have been described for nAChR in cortical thymus epithelial cell lines (Rinner *et al.*, 1994) and in mesothelioma cells, which may act via induction of NF-κB complexes and phosphorylation of Bad at serine (112). In this system, curare leads to apoptosis via p21 (waf-1)-dependent but p53-independent G(0)–G(1) arrest (Trombino *et al.*, 2004). On the other hand, 24 hour exposure of human dermal fibroblast (HDF) to 10 μM nicotine causes a 1.7- to 2-fold increase of the apoptosis regulators Bcl-2 and caspase 3, an effect suggested to be mediated by α3* nAChR (Arredondo *et al.*, 2003) and may be explained by calcium overload after overstimulation of cholinergic receptors, a mechanism observed in neural cells (Szabadkai and Rizzuto, 2004). In the epidermis, apoptosis has been proposed to be a central mechanism in the transition of differentiating keratinocytes from the stratum granulosum to the stratum corneum, a process termed ''apoptotic secretion'' and mediated by cholinergic receptors, most probably the α7-nAChR, present in the stratum granulosum. In this case, CD95 and Bax seem to be centrally involved (Arredondo *et al.*, 2003). In our system, we were not able to corroborate this finding, which however, may be due to the duration of the organotypical culture and hence the degree of cornification. Most notably, neither nicotine- nor α-bungarotoxin-treated cultures displayed increased apoptotic activity, CD95, or Bax upregulation.

Another important aspect in our study was the impact of the cholinergic system on epidermal differentiation and barrier formation. Starting with a thorough examination and quantification of the obtained epithelial thickness, we could show that in our system, the use of both mecamylamine and atropine led to a significantly delayed or impaired epidermal maturation as evidenced by reduced expression of typical markers of terminal differentiation like CK2e, CK10, filaggrin, Dsc1, and ZO-1. In contrast, we found a significantly increased epithelial thickness after treatment with cholinergic agonists. Nicotine produced the most impressive increase in epithelial thickness, whereas the effects observed for muscarine and carbachol were less pronounced. An increased polarity could be demonstrated for all cholinergic agonists. In hyperproliferative skin diseases, such as skin cancer or psoriasis vulgaris, and in normal keratinocytes forced into more frequent cell cycles, the polarized expression of integrins is lost, and α5β1 integrins becomes constitutively expressed on the plasma membrane (De Luca *et al.*, 1994). Control OTCs have been shown in several studies to be in a hyperproliferative or activated state, as indicated by the expression of CK 6/16. Likewise, in our control OTCs, α6- and β1-integrins were located in the basal and lower suprabasal layers. With increasing maturation, both integrins become increasingly restricted to the basal keratinocytes,

a phenomenon we could observe in OTCs treated with either cholinergic agonist. The restriction of integrin expression as well as keratinocyte proliferation to the basal layer upon stimulation with cholinergic agonists underlined the restored tissue polarity (Stark *et al.*, 2004b).

Using antibodies against Ki-67, we could not demonstrate an acceleration of epidermal differentiation, for example, on day 5 or 7 as compared to control; however, OTCs treated with cholinergic antagonists, displayed a significantly reduced proliferative activity.

It is well established, that keratinocytes grow better in culture if choline is present and hence virtually all culture media for keratinocytes contain $\sim 10^{-4}$ to 10^{-5} M choline-chloride. Thus, our results support this view of cholinergic agonists acting as a sort of trophic factor for keratinocyte growth and differentiation (Gordon *et al.*, 1988). The lipid content of the stratum corneum did not differ significantly between control and OTCs treated with cholinergic agonists. However, an interesting finding was the premature intracellular production of lipids already in the lower suprabasal layers, after treatment with cholinergic antagonists. Premature intracellular lipid production is a marker of abnormal keratinization and/or a hyperproliferative effect. In addition, it has been described after treatment of human skin with different agents such as retinoids, SDS, dithranol, UVB-irradiation, peroxisome proliferator-activated receptor activators and others (Kanerva, 1990; Feldman *et al.*, 1991; Schmuth *et al.*, 2004). This finding has been interpreted as stress or defense reaction to restore epidermal barrier integrity (Grubauer *et al.*, 1989; Holleran *et al.*, 1991; Corsini *et al.*, 2003). Interestingly, in rat adipocytes, a direct link between nAChR and lipid production has been demonstrated (Liu *et al.*, 2004). The inflammatory skin diseases, psoriasis, and atopic dermatitis also show impaired barrier function, but the underlying mechanisms remain under investigation. Recent studies in genetically engineered mice have suggested an unexpected role for tight junctions in epidermal barrier function (Madison, 2003). This is well in line with our observation of a significantly extended distribution of the tight junction protein ZO-1 in OTCs treated with cholinergic agonists. An extension of tight junction to spinous layers can be interpreted as a tightening of the epidermal barrier.

We used pharmacological cholinergic compounds to selectively stimulate or inhibit AChR, thus mimicking the biological process in which ACh and choline are the natural ligands and AChRs are either functional or not. The traditional view of cholinergic compounds has changed considerably in recent years, with the use of more refined electrophysiological and molecular biology methods. According to recent studies in different biological systems, mecamylamine, *d*-tubocurarine, and hexamethonium non-competitively block α3*- and α7-nAChR, with mecamylamine being the strongest inhibitor at the α3*-nAChR. D-tubocurarine displays greater affinity to the α3β4-nAChR than hexamethonium, whereas both show corresponding affinities at the α3β2-nAChR. At the concentration of 1 mM used in our study, about 50% of α7-nAChRs are blocked by mecamylamine. Mecamylamine is proposed to have

inhibiting activity at the α9-nAChR, a quantification of this activity has – to our knowledge – not been published. The lack of acantholytic activity of hexamethonium and D-tubocurarine may primarily be explained by their insufficient inhibitory action at the α9-nAChR, whereas for α-bungarotoxin the most likely explanation is due to its Mw of ~ 8 kDa, insufficient diffusion through the collagen gel (Xiao *et al.*, 1998; Verbitsky *et al.*, 2000). Atropine has traditionally been viewed as antimuscarinergic agent, however, recent studies have provided a rather pancholinergic inhibitory action in the rank order mAChR $>$α9->α7->α3-nAChR (Zwart and Vijverberg, 1997). In contrast to all other AChR, neither nicotine nor muscarine act as agonists at the α9nAChR, whereas ACh and choline are endogenous agonists and carbachol is a synthetic partial agonist (Verbitsky *et al.*, 2000).

Adding the pharmacological profile for the cholinergic substances used, to the distribution of the AChR in the epidermis and OTC of different developmental stages, it is most likely that inhibition of either α3*- or α9nAChR, which are both expressed in the basal and lower suprabasal layers, is necessary to induce acantholysis. In addition, inhibition of at least the stimulatory M_3 AChR, possibly also the M_5 AChR, which are both found in the basal layer, seems to produce similar effects. In contrast, predominant inhibition of the M_1 AChR by glycopyrrolate did not lead to acantholysis but disturbed epithelial architecture in the upper epidermal layers, thus interfering with barrier formation. These conclusions are supported by recent findings using knockout and gene-silencing approaches (Nguyen *et al.*, 2004b).

In conclusion, we could demonstrate an essential role for ACh in epidermal physiology. Our functional data provide insight into cholinergic control mechanisms of keratinocyte adhesion, differentiation, and barrier formation, the sum of which is likely to be involved in several skin diseases. The exact mechanisms, especially the role of the different AChR subunits, remain to be determined.

MATERIALS AND METHODS

Tissues
Normal human adult skin from the margins of routine surgical procedures and skin biopsies from patients with psoriasis, pemphigus vulgaris, and basal cell carcinoma were obtained after informed consent according to the Declaration of Helsinki Principles and approved by the local ethical committee. Samples were frozen in isopentane cooled in liquid nitrogen immediately after removal and stored at $-80°C$. Fresh samples were used to isolate normal epidermal keratinocytes and HDFs.

Cell culture
HDFs and normal epidermal keratinocytes were isolated from skin specimens as described (Stark *et al.*, 1999). HDFs were grown in DMEM (Bio Whittacker, Heidelberg, Germany) supplemented with 10% fetal calf serum. For OTCs, either senescent HDF of passages >10 or mitomycin C (8 μg/ml; Sigma, Steinheim, Germany)-treated HDF or X-irradiated (70 Gy) HDF were used. Normal epidermal keratinocytes were grown on feeder HDF in FAD medium (DMEM: Ham's F12/3:1) with 100 U/ml penicillin, 100 μg/ml streptomycin, and supplemented with 5% fetal calf serum, 5 μg/ml insulin, 1 ng/ml

recombinant epidermal growth factor, 10^{-10} M cholera toxin, 10^{-4} M adenine, and 0.4 µg/ml hydrocortisone (Sigma) as described (Stark *et al.*, 2004a).

OTCs

Lyophilized collagen type I was resolubilized at 4 mg/ml in 0.1% acetic acid and kept at 4°C. Collagen from different sources was used in parallel experiments without any obvious differences detectable. Rat tail collagen was either hand-isolated or bought from Sigma, calf skin collagen I was obtained from IBFB (Leipzig, Germany). The ice-cold collagen solution was mixed with Hank's salt with phenol red (Seromed Biochrom KG, Berlin, Germany) and adjusted to pH 7.4. The HDFs were resuspended in fetal calf serum and added to the gel to give 10^5 cells/ml in the collagen gel under cautious stirring. A 2.5 ml of the collagen/HDF solution was poured onto filter inserts (3 µm pore size, BD Falcon, Becton Dickinson, Heidelberg, Germany) of a 6-fold deep well plate (BioCoat, Becton-Dickinson, Heidelberg, Germany). After gelation, glass rings were mounted on the gels in order to define the area of epithelial cell growth. The gels were equilibrated by complete immersion in culture medium for 24–48 hours. Thereafter, the normal epidermal keratinocytes were plated inside the glass rings at a density of 10^6 cells/well. After 2 days, the glass rings were carefully removed and the medium level was lowered to the lower part of the gel, thus raising the keratinocytes to the air–liquid interface and restricting nourishment to diffusion from below. The air lift procedure is defined as day 0 of OTC. OTCs were grown in FAD medium with 10% fetal calf serum and 50 µM ascorbic acid. Medium was changed every 2–3 days. Alternatively, OTC were grown under serum-free conditions from day 0 as described (Stark *et al.*, 1999) using keratinocyte-defined medium (Promocell, Heidelberg, Germany) without pituitary extract containing 5 µg insulin/ml, 0.5 mg hydrocortisone/ml, 0.1 ng/ml human recombinant epidermal growth factor, 20 µg/ml transferrin (Promocell), 0.1% highly purified BSA (Vitromex, Selters, Germany), 50 µg/ml L-ascorbic acid, adjusted to 1.3 mM Ca^{2+}. At the end of the experiment, the epidermal-collagen specimens were snap frozen in liquid nitrogen and stored at −80°C.

In a single experiment, OTCs of one condition were always performed twice. All cell culture experiments were repeated at least twice. Cholinergic compounds were added to the OTCs on the day of the air-lift in concentrations ranging from 10 µM to 1 mM. We used nicotine as stimulus for the nAChR, muscarine as stimulus mAChR, and carbachol (carbamoylcholine chloride) as pancholinergic stimulus. Mecamylamine, hexamethonium, and *d*-tubocurarine were used to non-competitively block nAChR, α-bungarotoxin was used to reversibly block the homooligomeric nAChR, strychnine was used to block α9nAChR. mAChR were blocked by atropine and glycopyrrolate (which has 100 × times higher affinity to m1 than to m2 and m3). All cholinergic substances were from Sigma.

Determination of epithelial thickness

The epithelial thickness obtained using the described culture conditions was determined by measuring the thickness of the malpighian layer at two representative points of each specimen, so that for each condition, at least six different values were obtained. Statistical analysis was performed using Student's *t*-test (available on www.statpages.net).

LDH release assay

Cell death leads to release of cytoplasmic proteins into the culture supernatant. The determination of LDH is a well-established marker of cytotoxic effects in cell culturing (Weyermann *et al.*, 2005). We used the cytotoxicity detection kit (Roche, Mannheim, Germany) according to the manufacturer's instructions and determined LDH concentration in the culture supernatant at different time points. As positive control, a corresponding number of keratinocytes of were lysed using 1% Triton X-100.

IF staining

For IF analysis, 5 µm cryostat sections of human scalp skin were either used air dried and unfixed or fixed either in ice-cold acetone. IF reactions were performed at least three times on different specimens according to standard procedures (Kurzen *et al.*, 2004). After blocking with 5% non-fat dry milk and 1% BSA in Tris-buffered saline, the primary antibodies were applied to the specimens for 1 hour at room temperature or for 12 hours at 4°C. The following secondary antibodies were applied for 1 hour at room temperature: Cy-2 and Cy-3 coupled preabsorbed goat anti-mouse, -rabbit and -guinea-pig antisera and a Cy-3 coupled rabbit anti-goat antiserum, all obtained from Dianova (Hamburg, Germany). In order to enhance the signal intensity, biotin-coupled secondary antibodies were used. Antibody binding was visualized with Cy-2- or Cy-3-coupled streptavidin (Dianova). Negative controls were performed by replacing the primary antibody with phosphate-buffered saline or an irrelevant, species-matched antibody. Washes (3 × 10 minutes) in phosphate-buffered saline or Tris-buffered saline and Tween 20 were performed after each step. The staining was observed and visualized with a Leitz DMRB IF microscope. Antibodies used in the study are listed in Table 2.

Nile red staining

In order to better discern stratum corneum lipids, alkaline expansion was performed for 10 minutes using half-strength Sorensen–Walbum buffer (0.1 M glycine, 0.1 M NaCl, and 0.1 M NaOH) pH 10 or pH 12.5 as described (Talreja *et al.*, 2001) and gently rinsed with water. A Nile red stock solution containing 0.05% (wt/vol) Nile red in acetone was stored at 4°C. Before staining, the stock was diluted to 2.5 µg/ml with 75:25 (vol/vol) glycerol:water (Fowler and Greenspan, 1985). A drop of the glycerol–dye solution was applied to each section and immediately covered with a coverslip. Nile red fluorescence was captured with a Leitz microscope equipped with a fluorescein filter (450–490 nm excitation filter).

TUNEL assay

In order to detect apoptotic cells, we used the *in situ* cell death detection kit according to the manufacturer's (Roche) description. In brief, 5 µm thick frozen specimens were cut and fixed in 4% paraformaldehyde. After rinsing in phosphate-buffered saline, sections were permeabilized for 2 minutes. The TUNEL reaction mix was added to the sections and incubated for 60 minutes at 37°C. After thorough washing, nuclei were counterstained with 4′,6-diamidine-2′-phenylindole dihydrochloride (10 minutes at room temperature) washed again and mounted with fluoromount (Dako, Denmark). Positive control sections were pretreated with DNAse I.

Table 2. Antibodies used

Antigen	Antibody	Species	Source/reference
α3nAChR	GP5b	Guinea-pig	Kurzen *et al.* (2004)
α7nAChR	GP 9a	Guinea-pig	Kurzen *et al.* (2004)
α9nAChR	GPT1	Guinea-pig	Kurzen *et al.* (2004)
M_1 mAChR	AS-3701S	Rabbit	Biotrend
M_3 mAChR	AS-3741	Rabbit	Biotrend
M_5 mAChR	GP12b	Guinea-pig	Kurzen *et al.* (2004)
Desmocollin 1	Dsc1-U100	Mouse	Progen
Desmocollin 2	Rab 36	Rabbit	Progen
Desmoglein 1	Dsg1-P124	Mouse	Progen
Desmoglein 3	Dsg3-G194	Mouse	Progen
Desmoplakin	DP 2.17	Mouse	Progen
Plakoglobin	PG 5.17	Mouse	Progen
Laminin	Polyclonal	Rabbit	Progen
CK2e	Ks2.342.7.1	Mouse	Progen
CK19	Ks 19.1	Mouse	Progen
CK5/6	mab 17133	Mouse	Abcam, Cambridge, UK
CK16	mab NCL-CK16	Mouse	Novocastra
CK10	mab DEK-10	Mouse	DakoCytomation, Denmark
Filaggrin	mab FLG01	Mouse	Lab Vision, Fremont
E-cadherin	mab clone 36	Mouse	Transduction Laboratories, NH
β-Catenin	Clone 14	Mouse	Transduction Lab
γ-Catenin	Clone 15	Mouse	Transduction Lab
α6 Integrin	mab 1982	Mouse	Chemicon
β1-Integrin	Clone 20	Mouse	Immunotech, Marseille
ZO-1	—	Mouse	Zymed, Berlin, Germany
Claudin 4	RB-9266	Rabbit	Lab Vision, Phoenix, AZ
Activated caspase 3	ab 2302	Rabbit	Abcam
Caspase 8	mab C-15	Mouse	Kindly provided by P.H. Krammer, German Cancer Research Center, Heidelberg, Germany
Bax	mab 2D2	Mouse	Zymed
CD95	mab 95C03	Mouse	Chemicon, Munich, Germany
Ki-67	MIB-1	Mouse	DakoCytomation

AchR, acetylcholine receptor.

RNA isolation and cDNA synthesis

For RNA isolation, the epithelial sheets were separated from the collagen matrix and the RNA was isolated using RNeasy Mini kit (Qiagen, Hilden, Germany) according to the recommendations of the manufacturer. Total RNA was treated with 2 U RNase free DNase (Ambion, Austin, TX) and used for RT with Superscript™ II reverse transcriptase (Invitrogen, Karlsruhe, Germany) using oligo dT primers according to the recommendations of the manufacturer. The obtained cDNA was diluted 1:10 with DDH$_2$O and 1 μl was used for PCR reaction.

Real-time RT-PCR analysis

Real-time PCR analysis was performed using Assay-on-Demand® TaqMan® assays together with TaqMan® PCR master mix (all from Applied Biosystems, Darmstadt, Germany) using standard conditions. The following assays have been used: for α9nAChR (CHRNA9) Hs00214034_m1, for desmoglein 3 – Hs00170075_m1, for E-cadherin Hs00170423_m1. As internal control, an assay for human GAPDH was used together with TaqMan® PCR master mix (Applied Biosystems). Primers for GAPDH were: forward – F848 5′-CATCCATGACAACTTTGGTATCGT; reverse – R848 5′-CAGTCTTCTGGGTGGCAGTGA. The probe for GAPDH was Pr849 FAM-AAGGACTCATGACCACAGTCCATGCC-BHQ1. Probe and primers were produced by MWG-Biotech (Ebersberg, Germany). The experiments were performed on ABI PRISM® 7000 sequence detection system (Applied Biosystems). The expression levels of analyzed genes were normalized to GAPDH mRNA expression.

CONFLICT OF INTEREST

The authors state no conflict of interest.

REFERENCES

Amagai M (2003) Desmoglein as a target in autoimmunity and infection. *J Am Acad Dermatol* 48:244–52

Amagai M, Klaus-Kovtun V, Stanley JR (1991) Autoantibodies against a novel epithelial cadherin in pemphigus vulgaris, a disease of cell adhesion. *Cell* 67:869–77

Anderson JM, Van Itallie CM (1995) Tight junctions and the molecular basis for regulation of paracellular permeability. *Am J Physiol* 269(Part 1):G467–75

Aoyama Y, Kitajima Y (1999) Pemphigus vulgaris-IgG causes a rapid depletion of desmoglein 3 (Dsg3) from the Triton X-100 soluble pools, leading to the formation of Dsg3-depleted desmosomes in a human squamous carcinoma cell line, DJM-1 cells. *J Invest Dermatol* 112:67–71

Arredondo J, Hall LL, Ndoye A, Nguyen VT, Chernyavsky AI, Bercovich D *et al.* (2003) Central role of fibroblast alpha3 nicotinic acetylcholine receptor in mediating cutaneous effects of nicotine. *Lab Invest* 83:207–25

Arredondo J, Nguyen VT, Chernyavsky AI, Bercovich D, Orr-Urtreger A, Vetter DE *et al.* (2002) Central role of alpha7 nicotinic receptor in differentiation of the stratified squamous epithelium. *J Cell Biol* 159:325–36

Brenner S, Ruocco V, Bialy-Golan A, Tur E, Flaminio C, Ruocco E *et al.* (1999) Pemphigus and pemphigoid-like effects of nifedipine on *in vitro* cultured normal human skin explants. *Int J Dermatol* 38:36–40

Buchli R, Ndoye A, Arredondo J, Webber RJ, Grando SA (2001) Identification and characterization of muscarinic acetylcholine receptor subtypes expressed in human skin melanocytes. *Mol Cell Biochem* 228:57–72

Corsini E, Viviani B, Zancanella O, Lucchi L, Visioli F, Serrero G *et al.* (2003) Induction of adipose differentiation related protein and neutral lipid droplet accumulation in keratinocytes by skin irritants. *J Invest Dermatol* 121:337–44

De Luca M, Pellegrini G, Zambruno G, Marchisio PC (1994) Role of integrins in cell adhesion and polarity in normal keratinocytes and human skin pathologies. *J Dermatol* 21:821–8

Dhitavat J, Cobbold C, Leslie N, Burge S, Hovnanian A (2003) Impaired trafficking of the desmoplakins in cultured Darier's disease keratinocytes. *J Invest Dermatol* 121:1349–55

Elgoyhen AB, Johnson D, Boulter J, Vetter DE, Heinemann S (1994) α9: an acetylcholine receptor with novel pharmacological properties expressed in rat cochlear hair cells. *Cell* 79:705–15

Feldman D, Bryce GF, Shapiro SS (1991) Ultrastructural effects of UVB radiation and subsequent retinoic acid treatment on the skin of hairless mice. *J Cutan Pathol* 18:46–55

Fowler SD, Greenspan P (1985) Application of Nile red, a fluorescent hydrophobic probe, for the detection of neutral lipid deposits in tissue sections: comparison with oil red O. *J Histochem Cytochem* 33:833–6

Frisch SM, Francis H (1994) Disruption of epithelial cell–matrix interactions induces apoptosis. *J Cell Biol* 124:619–26

Fuchs E (1990) Epidermal differentiation. *Curr Opin Cell Biol* 2:1028–35

Gordon PR, Gelman LK, Gilchrest BA (1988) Demonstration of a choline requirement for optimal keratinocyte growth in a defined culture medium. *J Nutr* 118:1487–94

Grando SA (1997) Biological functions of keratinocyte cholinergic receptors. *J Investig Dermatol Symp Proc* 2:41–8

Grando SA (2000) Autoimmunity to keratinocyte acetylcholine receptors in pemphigus. *Dermatology* 201:290–5

Grando SA (2004) New approaches to the treatment of pemphigus. *J Investig Dermatol Symp Proc* 9:84–91

Grando SA, Horton RM, Pereira EF, Diethelm-Okita BM, George PM, Albuquerque EX *et al.* (1995a) A nicotinic acetylcholine receptor regulating cell adhesion and motility is expressed in human keratinocytes. *J Invest Dermatol* 105:774–81

Grando SA, Pittelkow MR, Shultz LD, Dmochowski M, Nguyen VT (2001) Pemphigus: an unfolding story. *J Invest Dermatol* 117:990–5

Grando SA, Zelickson DB, Kist DA, Weinshenker D, Bigliardi PL, Wendelschafer CG *et al.* (1995b) Keratinocyte muscarinic acetylcholine receptors: immunolocalization and partial characterization. *J Invest Dermatol* 104:95–100

Grubauer G, Feingold KR, Harris RM, Elias PM (1989) Lipid content and lipid type as determinants of the epidermal permeability barrier. *J Lipid Res* 30:89–96

Hakuno M, Shimizu H, Akiyama M, Amagai M, Wahl JK, Wheelock MJ *et al.* (2000) Dissociation of intra- and extracellular domains of desmosomal cadherins and E-cadherin in Hailey–Hailey disease and Darier's disease. *Br J Dermatol* 142:702–11

Hashimoto K, Fujiwara K, Tada J, Harada M, Setoyama M, Eto H (1995) Desmosomal dissolution in Grover's disease, Hailey–Hailey's disease and Darier's disease. *J Cutan Pathol* 22:488–501

Hermiston ML, Gordon JI (1995) *In vivo* analysis of cadherin function in the mouse intestinal epithelium: essential roles in adhesion, maintenance of differentiation, and regulation of programmed cell death. *J Cell Biol* 129:489–506

Hertl M, Veldman C (2001) Pemphigus – paradigm of autoantibody-mediated autoimmunity. *Skin Pharmacol Appl Skin Physiol* 14:408–18

Holleran WM, Man MQ, Gao WN, Menon GK, Elias PM, Feingold KR (1991) Sphingolipids are required for mammalian epidermal barrier function. Inhibition of sphingolipid synthesis delays barrier recovery after acute perturbation. *J Clin Invest* 88:1338–45

Kanerva L (1990) Electron microscopy of the effects of dithranol on healthy and on psoriatic skin. *Am J Dermatopathol* 12:51–62

Kirkpatrick CJ, Bittinger F, Nozadze K, Wessler I (2003) Expression and function of the non-neuronal cholinergic system in endothelial cells. *Life Sci* 72:2111–6

Kurzen H, Berger H, Jäger C, Hartschuh W, Näher H, Gratchev A *et al.* (2004) Phenotypical and molecular profiling of the extraneuronal cholinergic system of the skin. *J Invest Dermatol* 123:937–49

Kurzen H, Jung EG, Hartschuh W, Moll I, Franke WW (1999) Forms of epithelial differentiation of draining sinus in acne inversa. *Br J Dermatol* 141:231–9

Kurzen H, Schallreuter KU (2004) Novel aspects in cutaneous biology of acetylcholine synthesis and acetylcholine receptors. *Exp Dermatol* 13(Suppl 4):27–30

Leloup C, Michaelson DM, Fisher A, Hartmann T, Beyreuther K, Stein R (2000) M1 muscarinic receptors block caspase activation by phosphoinositide 3-kinase- and MAPK/ERK-independent pathways. *Cell Death Differ* 7:825–33

LeSagE G, Alvaro D, Benedetti A, Glaser S, Marucci L, Baiocchi L *et al.* (1999) Cholinergic system modulates growth, apoptosis, and secretion of cholangiocytes from bile duct-ligated rats. *Gastroenterology* 117:191–9

Liu RH, Mizuta M, Matsukura S (2004) The expression and functional role of nicotinic acetylcholine receptors in ratadipocytes. *J Pharmacol Exp Ther* 310:52–8

Lo Schiavo A, Guerrera V, Cozzani E, Aurilia A, Ruocco E, Pinto F (1999) *In vivo* enalapril-induced acantholysis. *Dermatology* 198:391–3

Madison KC (2003) Barrier function of the skin: ''la raison d'etre'' of the epidermis. *J Invest Dermatol* 121:231–41

Millar N (2003) Assembly and subunit diversity of nicotinic acetylcholine receptors. *Biochem Soc Trans* 31:869–74

Ndoye A, Buchli R, Greenberg B, Nguyen VT, Zia S, Rodriguez JG *et al.* (1998) Identification and mapping of keratinocyte muscarinic acetylcholine receptor subtypes in human epidermis. *J Invest Dermatol* 111:410–6

Nguyen VT, Arredondo J, Chernyavsky AI, Kitajima Y, Grando SA (2003) Keratinocyte acetylcholine receptors regulate cell adhesion. *Life Sci* 72:2081–5

Nguyen VT, Arredondo J, Chernyavsky AI, Pittelkow MR, Kitajima Y, Grando SA (2004a) Pemphigus vulgaris acantholysis ameliorated by cholinergic agonists. *Arch Dermatol* 140:327–34

Nguyen VT, Chernyavsky AI, Arredondo J, Bercovich D, Orr-Urtreger A, Vetter DE *et al.* (2004b) Synergistic control of keratinocyte adhesion through muscarinic and nicotinic acetylcholine receptor subtypes. *Exp Cell Res* 294:534–49

Nguyen VT, Lee TX, Ndoye A, Shultz LD, Pittelkow MR, Dahl MV *et al.* (1998) The pathophysiological significance of nondesmoglein targets of Pemphigus autoimmunity. Development of antibodies against keratinocyte cholinergic receptors in patients with pemphigus vulgaris and pemphigus foliaceus. *Arch Dermatol* 134:971–80

Nguyen VT, Ndoye A, Grando SA (2000a) Novel human alpha9 acetylcholine receptor regulating keratinocyte adhesion is targeted by Pemphigus vulgaris autoimmunity. *Am J Pathol* 157:1377–91

Nguyen VT, Ndoye A, Hall LL, Zia S, Arredondo J, Chernyavsky AI *et al.* (2001) Programmed cell death of keratinocytes culminates in apoptotic secretion of a humectant upon secretagogue action of acetylcholine. *J Cell Sci* 114:1189–204

Nguyen VT, Ndoye A, Shultz LD, Pittelkow MR, Grando SA (2000b) Antibodies against keratinocyte antigens other than desmogleins 1 and 3 can induce pemphigus vulgaris-like lesions. *J Clin Invest* 106:1467–79

Presland RB, Jurevic RJ (2002) Making sense of the epithelial barrier: what molecular biology and genetics tell us about the functions of oral mucosal and epidermal tissues. *J Dent Educ* 66:564–74

Reed JC (2000) Mechanisms of apoptosis. *Am J Pathol* 157:1415–30

Rinner I, Kukulansky T, Felsner P, Skreiner E, Globerson A, Kasai M *et al.* (1994) Cholinergic stimulation modulates apoptosis and differentiation of murine thymocytes via a nicotinic effect on thymic epithelium. *Biochem Biophys Res Commun* 203:1057–62

Schmidt E, Brocker EB, Zillikens D (2000) Pemphigus. Loss of desmosomal cell–cell contact. *Hautarzt* 51:309–18

Schmuth M, Haqq CM, Cairns WJ, Holder JC, Dorsam S, Chang S *et al.* (2004) Peroxisome proliferator-activated receptor (PPAR)-beta/delta stimulates differentiation and lipid accumulation in keratinocytes. *J Invest Dermatol* 122:971–83

Segre J (2003) Complex redundancy to build a simple epidermal permeability barrier. *Curr Opin Cell Biol* 15:776–82

Seguela P, Wadiche J, Dineley-Miller K, Dani JA, Patrick JW (1993) Molecular cloning, functional properties, and distribution of rat brain alpha 7: a nicotinic cation channel highly permeable to calcium. *J Neurosci* 13:596–604

Setoyama M, Choi KC, Hashimoto K, Ishihara M, Predeteanu GS, Dinehart S *et al.* (1991) Desmoplakin I and II in acantholytic dermatoses:

preservation in pemphigus vulgaris and pemphigus erythematosus and dissolution in Hailey–Hailey's disease and Darier's disease. *J Dermatol Sci* 2:9–17

Sgard F, Charpentier E, Bertrand S, Walker N, Caput D, Graham D *et al.* (2001) A novel human nicotinic receptor subunit, α10, that confers functionality to the α9-subunit. *Mol Pharmacol* 61:150–9

Smith EW, Smith KA, Maibach HI, Andersson PO, Cleary G, Wilson D (1992) The local side effects of transdermally absorbed nicotine. *Skin Pharmacol* 5:69–76

Stanley JR, Nishikawa T, Diaz LA, Amagai M (2001) Pemphigus: is there another half of the story? *J Invest Dermatol* 116:489–90

Stark HJ, Baur M, Breitkreutz D, Mirancea N, Fusenig NE (1999) Organotypic keratinocyte cocultures in defined medium with regular epidermal morphogenesis and differentiation. *J Invest Dermatol* 112:681–91

Stark HJ, Szabowski A, Fusenig NE, Maas-Szabowski N (2004a) Organotypic cocultures as skin equivalents: a complex and sophisticated *in vitro* system. *Biol Proc Online* 6:55–60

Stark HJ, Willhauck MJ, Mirancea N, Boehnke K, Nord I, Breitkreutz D *et al.* (2004b) Authentic fibroblast matrix in dermal equivalents normalises epidermal histogenesis and dermoepidermal junction in organotypic co-culture. *Eur J Cell Biol* 83:631–45

Szabadkai G, Rizzuto R (2004) Participation of endoplasmic reticulum and mitochondrial calcium handling in apoptosis: more than just neighborhood? *FEBS Lett* 567:111–5

Talreja P, Kleene NK, Pickens WL, Wang TF, Kasting GB (2001) Visualization of the lipid barrier and measurement of lipid pathlength in human stratum corneum. *AAPS Pharm Sci* 3:E13, 1–9

Trombino S, Bisio A, Catassi A, Cesario A, Falugi C, Russo P (2004) Role of the non-neuronal human cholinergic system in lung cancer and mesothelioma: possibility of new therapeutic strategies. *Curr Med Chem Anti-Canc Agents* 4:535–42

van Koppen CJ, Kaiser B (2003) Regulation of muscarinic acetylcholine receptor signaling. *Pharmacol Ther* 98:197–220

Verbitsky M, Rothlin CV, Katz E, Elgoyhen AB (2000) Mixed nicotinic–muscarinic properties of the alpha9 nicotinic cholinergic receptor. *Neuropharmacology* 39:2515–24

Wang X, Bregegere F, Frusic-Zlotkin M, Feinmesser M, Michel B, Milner Y (2004) Possible apoptotic mechanism in epidermal cell acantholysis induced by pemphigus vulgaris autoimmunoglobulins. *Apoptosis* 9:131–43

Weyermann J, Lochmann D, Zimmer A (2005) A practical note on the use of cytotoxicity assays. *Int J Pharm* 288:369–76

Xiao Y, Meyer EL, Thompson JM, Surin A, Wroblewski J, Kellar KJ (1998) Rat alpha3/beta4 subtype of neuronal nicotinic acetylcholine receptor stably expressed in a transfected cell line: pharmacology of ligand binding and function. *Mol Pharmacol* 54:322–33

Zia S, Ndoye A, Lee TX, Webber RJ, Grando SA (2000) Receptor-mediated inhibition of keratinocyte migration by nicotine involves modulations of calcium influx and intracellular concentration. *J Pharmacol Exp Ther* 293:973–81

Zwart R, Vijverberg HP (1997) Potentiation and inhibition of neuronal nicotinic receptors by atropine: competitive and noncompetitive effects. *Mol Pharmacol* 52:886–95